Oil Shale, 2024, Vol. 41, No. 3, pp. 189–207
doi: https://doi.org/10.3176/oil.2024.3.03
ISSN 0208-189X

Study on the influence of non-temperature factors on the migration path of organic carbon and evolution characteristics of pore permeability parameters of organic-rich shale under supercritical water in situ conversion

Tian Xie[(a)]*, Qiuyang Zhao[(b)]*, Hui Jin[(b,c)], Yechun Wang[(b,c)], Liejin Guo[(b)]

[(a)] Xi'an Shiyou University, Xi'an 710065, China
[(b)] State Key Laboratory of Multiphase Flow in Power Engineering, Xi'an Jiaotong University, Xi'an 710049, China
[(c)] Xinjin Weihua Institute of Clean Energy Research, Foshan City 528216, China

Received 5 April 2024, accepted 12 July 2024, available online 5 August 2024

Abstract. *In this study, a non-isothermal heating reactor was used to simulate the hydrocarbon generation process of 1–4 cm sized medium- and low-maturity organic-rich shale under the action of supercritical water. The results show that the increase in pressure had a negative effect on the utilization of organic carbon in shale. As the pressure increased, the overall conversion efficiency of organic carbon decreased. Although higher pressure inhibited both oil and gas production, the inhibition of the gas production process was more significant. The effect of reaction time on oil and gas production differed in stages. Over a 4-h reaction period, the oil and gas production rates gradually increased with longer reaction times, with oil production showing a stronger promotion effect. Beyond 4 h, further extension of reaction time mainly promoted gas production. The increase in pressure and reaction time had opposite effects on the pore structure parameters of shale. Higher pressure led to a decrease in these parameters, while longer reaction times resulted in improved and expanded parameters.*

Keywords: *organic-rich shale, supercritical water, hydrocarbon generation, migration path, pore evolution.*

* Corresponding authors, xietian@xsyu.edu.cn, qyzhao@mail.xjtu.edu.cn

1. Introduction

In recent years, the depletion of traditional oil resources has intensified the focus on organic-rich shale, which contains abundant reserves of shale oil and gas. Various assessments by different institutions estimate China's geological resources of shale oil to be between 100 and 3722 × 10^8 billion tons, making it widely regarded as a strategic replacement for conventional oil [1]. Based on the maturity of organic matter, organic-rich shale can be roughly divided into two categories: medium- and high-maturity, and medium- and low-maturity shale. Resource endowment of the two determines their different development methods. For medium- and high-maturity organic-rich shale resources, the development bottleneck lies in poor seepage channels, hindering the extraction and use of oil and gas products. For medium- and low-maturity organic-rich shale resources, apart from poor seepage conditions, the difficulty in development is that internal organic matter exists in a solid form and cannot flow [2, 3]. Therefore, in order to efficiently develop organic-rich shale resources, it is necessary to convert internal solid organic matter into liquid or gaseous fluid through certain technical means.

Predecessors have invented technologies such as electric heating, fluid heating, radiation heating, and combustion heating to promote the evolution of hydrocarbon generation from kerogen [4–10]. These technologies can be divided into fluid and non-fluid heating technologies. Compared with non-fluid heating technology, the advantage of fluid heating technology is that it ensures high conversion efficiency as well as increases the elastic energy of the reservoir, which provides the energy driving foundation for the displacement development after conversion. Among these technologies, supercritical water conversion technology can simultaneously meet the development needs of medium- and low-maturity organic-rich shale with high conversion efficiency, high oil washing efficiency, and high swept volume, thus attracting wide attention [11, 12].

Supercritical water refers to water with temperature and pressure simultaneously exceeding the critical point (374 °C, 22.1 MPa), and with excellent physical and chemical properties, such as high reactivity, solubility and dispersion [13–15]. Leveraging these properties, supercritical water has been widely used in biomass treatment [16–18], fossil energy processing [19–21], organic waste management [22–24], and other processes. The carbon–carbon bond binding energy in oil molecules and the ring-opening free energy of polycyclic aromatic hydrocarbons can be reduced by more than 70% due to their high reaction characteristics, which creates favorable conditions for the upgrading of low-grade crude oil. Due to its high solubility, supercritical water can dissolve a large amount of organic matter, miscible with oil and gas in the process of oil and gas exploitation, increase the efficiency of oil washing, and further improve the recovery rate of crude oil. The high diffusion characteristics of supercritical water allow it to enter the micro- and nano-scale pore throats inaccessible to liquid water and normal water vapor, increase

the effective swept volume, and further improve the oil recovery. These characteristics indicate that supercritical water has significant advantages in porous media, such as percolation, heat and mass transfer, and promoting the evolution of organic matter to a mature state. Consequently, supercritical water holds promise for application in the development of medium- and low-maturity organic-rich shale resources.

Previous studies on hydrocarbon generation from organic-rich shale in supercritical water have been carried out [25–31], revealing temperature as the most critical factor affecting the process. It was observed that hydrocarbon generation efficiency initially increased and then decreased with rising temperature. However, the influence of temperature on the composition of product components was found to be closely related to the size of the shale particles involved in the reaction. For millimeter-sized granular shale, elevated temperatures promoted the gasification of organic matter and the production of light oil, whereas for centimeter-sized massive shale, higher temperatures promoted the production of heavy oil. This change in hydrocarbon generation mechanisms stemmed from the increase in shale size [32]. At the same time, it was inevitable that the pyrolysis of organic matter and inorganic minerals during hydrocarbon generation altered shale pores. Shale pore permeability parameters are crucial for controlling the efficient development of internal organic matter. Interestingly, previous studies found that the expansion of pores after increasing the temperature to 430 °C was not solely attributed to the pyrolysis of organic matter, but also to the development of micro-cracks on the shale surface under the action of thermal stress [12]. Therefore, the changes in porosity and permeability parameters do not follow a simple linear law but exhibit certain complexity.

In summary, the hydrocarbon generation process of organic-rich shale in a supercritical water environment is an extremely complex geochemical reaction process, where temperature plays a crucial role, but the influence of other non-temperature factors cannot be ignored. These non-temperature factors, such as pressure, reaction time, mineral composition, and water chemistry, may affect the conversion efficiency of organic matter and the formation of hydrocarbons to varying degrees. In the actual laboratory experiment and field practice, these factors are often intertwined to act on the hydrocarbon generation process of shale. While the influence of temperature on hydrocarbon generation has been widely studied, there are relatively few studies on non-temperature factors, especially the influence of pressure and reaction time on the migration path and pore structure of organic carbon. Hence, this study aims to investigate in detail the effects of pressure and reaction time on the migration path and pore evolution of organic carbon in hydrocarbon generation in supercritical water, focusing on medium- and low-maturity organic-rich shale and using carefully designed experiments.

In addition, this study represents a continuation and expansion of our team's previous research results on hydrocarbon generation from medium- and low-

maturity organic-rich shale in supercritical water. We hope that the findings of this study will contribute to a more scientific theoretical basis and practical guidance for the application of supercritical water technology in shale oil and gas development. In the future, we will continue to explore other factors that may affect the efficiency of hydrocarbon generation, and optimize the experimental conditions to achieve higher hydrocarbon generation efficiency and economic benefits, thus fostering the sustainable development of shale oil and gas resources.

2. Experiment

2.1. Experimental system

The experimental system employed in this research consisted of a high-temperature and high-pressure reactor made of Hastelloy alloy. The volume of the reactor chamber is about 80 mL, which can withstand temperatures up to 700 °C and pressures of up to 35 MPa.

2.2. Experimental procedure

During the shale oil extraction and analysis process, it was necessary to prepare an appropriate amount of shale samples and deionized water. These raw materials were mixed in a predetermined proportion and placed into a closed reactor, where they reacted under controlled temperature and pressure conditions. This process aimed to simulate the conditions of underground oil and gas generation, using chemical reactions to convert organic matter in shale into usable oil and gas resources. After the reaction was completed, the gas generated in the reactor was collected first by connecting a gas collection device to ensure the purity and accuracy of the gas sample. The gas was collected for subsequent gas chromatographic analysis, providing insights into its composition, including hydrocarbons and other possible compounds.

Next, the material from the reactor was transferred to a separation device, where the mixture was separated into an oil phase, a water phase, and a solid residue, using physical methods such as centrifugation or sedimentation. The oil phase contained liquid hydrocarbons extracted from shale, while the water phase contained water generated during the reaction along with other water-soluble substances. To ensure the accuracy of subsequent tests, the separated oil phase material and solid residue were dried. The oil phase material was dried at a constant temperature of 46 °C to remove any moisture. The solid residue was dried at a high temperature of 100 °C to ensure the removal of all moisture that could affect the test results.

After the drying process, the solid residue was used for elemental analysis and pore structure analysis. An element analyzer was employed to determine the content of each element in the solid residue, necessary for understanding the mineral composition and chemical properties of shale. A

mercury injection instrument was used to measure the pore structure of the solid residue, which was of great significance for evaluating the reservoir characteristics and hydrocarbon generation potential of shale. Gas samples were analyzed with a gas chromatograph, a technique capable of separating and quantifying the individual components in a complex gas mixture. Through gas chromatography, detailed information regarding the content and proportion of various hydrocarbons and other gas components in the gas sample was obtained. Aqueous substances were tested with a total organic carbon (TOC) tester, which measured the amount of TOC in water to assess the concentration of organic material in the aqueous phase. This was useful for understanding the dissolution and migration of organics during shale oil extraction.

Through this series of processing and testing steps, detailed information was obtained about shale samples, including the conversion efficiency of organic matter, the composition of oil and gas components, and reservoir characteristics. These data hold important reference value for the development and utilization of shale oil and gas resources. Detailed basic information of experimental samples, test steps, and calculation formulas have been reported in previous research work [12].

3. Results and discussion

3.1. Organic carbon migration during hydrocarbon generation

Kerogen is the main component of effective resources in low-maturity organic-rich shale, and it is an organic compound with complex structure. Due to the complexity of kerogen's structure and the limitation of testing methods under the current scientific and technological level, we have not been able to accurately obtain its chemical formula, so as to fully characterize the characteristics of kerogen. Therefore, it is challenging to describe the process of hydrocarbon generation in supercritical water by using a macroscopic material chemistry equation. However, we can shift our perspective and take a more simplified approach to the problem.

From an elemental perspective, the focus often lies on the organic carbon content in carbon-based fuels, which is also applicable to the study of medium- and low-maturity organic-rich shale. Organic carbon is a key component of organic matter in shale, and its abundance measurement has been widely accepted as an indicator to evaluate the content of organic matter in shale. In fact, the hydrocarbon generation process of medium- and low-maturity organic-rich shale in supercritical water can essentially be regarded as the pyrolysis process of complex compounds rich in organic carbon under high temperature and pressure, resulting in a variety of compounds containing organic carbon. Therefore, in the following discussion, we will explore the migration path of organic carbon elements in medium- and low-maturity organic-rich shale in supercritical water environment under the influence

of different non-temperature factors, and how these factors affect the transformation and distribution of organic carbon. Through this exploration, we endeavor to provide new insights into understanding and optimizing the process of shale oil and gas generation.

3.1.1. Influence of pressure on organic carbon migration

Figure 1 shows the relationship between the oil production rate and pressure, indicating a decrease in the oil production rate from 2.4 to 1.5 kg oil · t^{-1} shale as pressure increases from 22.5 to 27.5 MPa. Figure 2 illustrates the relationship between the gas production rate and pressure, demonstrating a decline in the gas production rate from 15.6 to 14.9 m^3 gas · t^{-1} shale with increasing pressure. Figure 3 shows the relationship between the quality of carbon in wastewater, its production rate, and pressure. Notably, as pressure increases from 22.5 to 27.5 MPa, both the quality and production rate of organic carbon in wastewater exhibit an upward trend. Figure 4 illustrates the relationship between the degree of organic carbon utilization and pressure, with the degree of organic carbon utilization decreasing from 5.69 to 5.19% as pressure rises from 22.5 to 27.5 MPa.

Based on the above results, it is evident that the increase in pressure is not conducive to the overall utilization of organic carbon, which may be caused by two reasons. First, increased pressure inhibits the release of oil and gas products generated from kerogen conversion within the internal space of shale pores to the supercritical water atmosphere outside shale. Second, the increase in pressure inhibits the formation path of gas products. For the equilibrium reaction, the increase in pressure is not conducive to the further development of the reaction path towards increased gas volume [29]. Figure 5 shows the variation of carbon sources in carbon dioxide with increasing pressure, revealing that pressure changes have little effect on whether the carbon in carbon dioxide comes from organic or inorganic sources. It can be inferred that the change of pressure has limited influence on the reaction path in the hydrocarbon generation reaction, and the increase in pressure mainly inhibits the further release of hydrocarbon generation products. The results depicted in Figure 5 clearly provide strong support for the first cause for the decline in the level of organic carbon utilization with increasing pressure.

Based on the results of oil, gas, and organic carbon production rates in wastewater, the relative proportion of organic carbon elements contained in the three-phase products of oil, gas and water under different pressure conditions was further calculated, as shown in Figure 6. It is evident that as pressure increases from 22.5 to 27.5 MPa, the proportion of organic carbon migrating to gas shows a decreasing trend, whereas the proportion of organic carbon migrating to oil and water exhibits an increasing trend. This indicates that the increase in pressure inhibits both oil and gas generation, with a stronger inhibiting effect on gas generation.

In our previous research work [11, 12], conducted under laboratory experimental conditions, the yield of organic matter distributed in wastewater after oil and gas generation of medium- and low-maturity organic-rich shale in supercritical water atmosphere was significantly lower than that in oil and gas phase products. For this reason, the yield of organic matter distributed in wastewater after the reaction is often ignored. However, for large organic-rich shale reservoirs in the field, this still requires sufficient attention. Combined with previous research results, it is evident that organic carbon in wastewater mainly comes from certain organic compounds with oxygen functional groups, such as cyclohexanone derivatives, isoparaffin and phenolic derivatives, normal alkanes, naphthenic acids, heteroatoms, and esters [33]. The results depicted in Figure 6 are fully consistent with the variation trend observed in the products of oil shale pyrolysis, as reported by earlier studies [27, 28], indicating that oil and gas products are the primary products, while water-soluble organic compounds are secondary products. Moreover, Figure 6 shows that with increasing pressure, the formation trend of water-soluble organic matter is stronger, and the increase in pressure also promotes the dissolution of a portion of organic matter in water. When the pressure returns to normal levels, the organic matter dissolved in water is difficult to desorb twice. Consequently, liquid water acts as a confining agent, leading to the formation of water-soluble organic matter and a gradual increase in water-soluble organic carbon content.

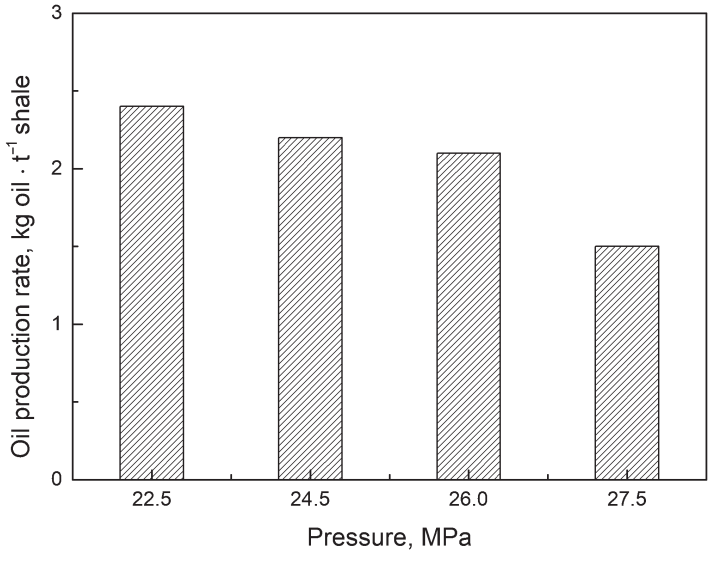

Fig. 1. Influence of pressure on oil production rate.

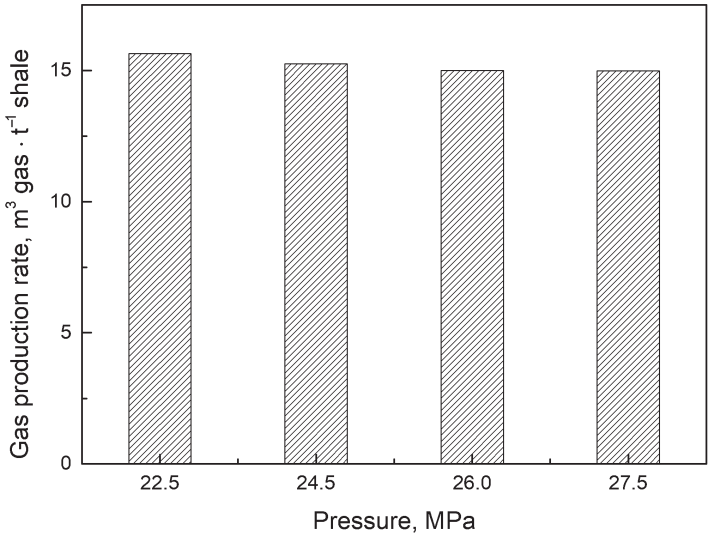

Fig. 2. Influence of pressure on gas production rate.

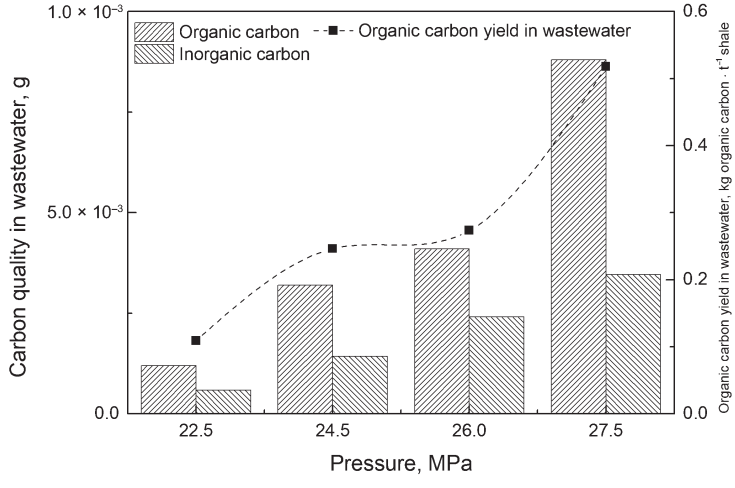

Fig. 3. Influence of pressure on carbon mass distribution in wastewater.

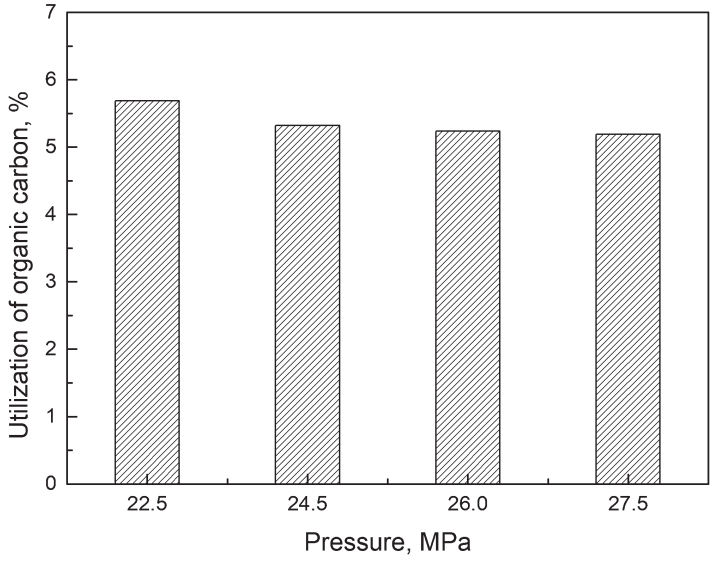

Fig. 4. Effect of pressure on the degree of organic carbon utilization.

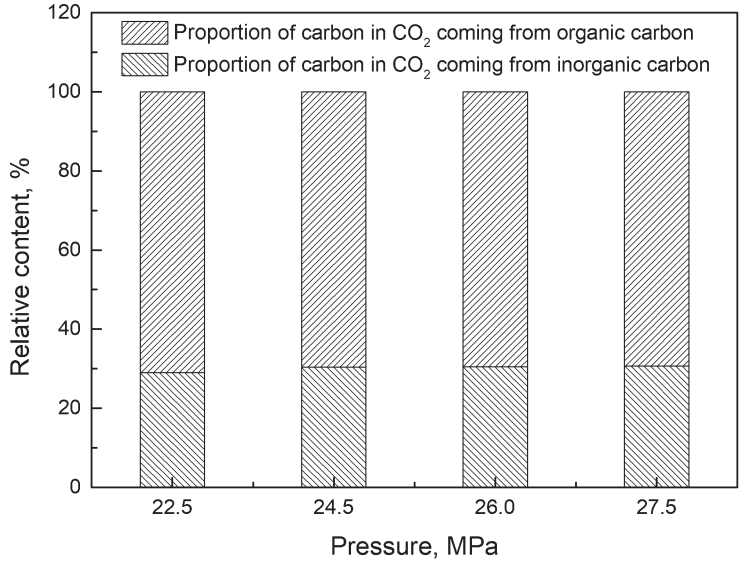

Fig. 5. Effect of pressure on carbon sources in carbon dioxide.

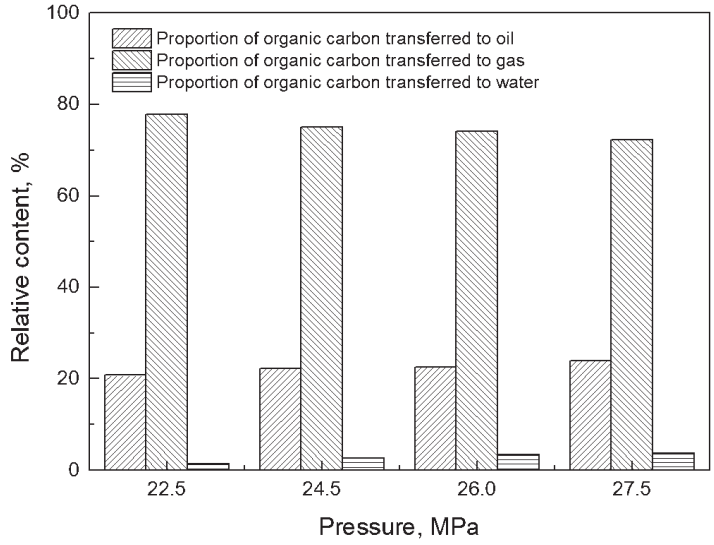

Fig. 6. Effect of pressure on organic carbon migration ratio.

3.1.2. Influence of reaction time on organic carbon migration

Figure 7 shows the relationship between the oil production rate and reaction time. When reaction time increases from 1 to 12 h, the oil production rate initially increases, reaching a peak of 3.65 kg oil · t^{-1} shale at 4 h, and then decreases. Figure 8 depicts the relationship between the gas production rate and reaction time, with the rate increasing from 15.6 to 27.6 m^3 gas · t^{-1} shale as reaction time extends from 1 to 12 h. Figure 9 illustrates the relationship between the quality of carbon in wastewater, its production rate, and reaction time. When reaction time increases from 1 to 12 h, both the quality of organic carbon in wastewater and its production rate increase first and then decrease. Figure 10 shows the relationship between the degree of organic carbon utilization and reaction time. The degree of organic carbon utilization rises from 5.69 to 16.9% with increasing time.

Figure 11 illustrates the change of carbon sources in carbon dioxide with reaction time. It is evident that the carbon mass from the organic part gradually decreases with increasing reaction time, whereas the carbon mass from the inorganic part gradually increases with longer reaction time. The reason is that this study did not involve the change of mass of the initial reactants with increasing time. The changing trend of organic matter production in wastewater is consistent with that of the oil phase product, showing an initial increase followed by a decrease with the increase in reaction time. Correspondingly, the quality of organic carbon in wastewater also increases first and then decreases with longer reaction time.

Figure 12 shows the distribution ratio of converted organic carbon in the three-phase products of oil, gas, and water during the hydrocarbon generation process of medium- and low-maturity organic-rich shale in supercritical water co-heated conditions with increasing reaction time. As evident, the distribution ratio of organic carbon in oil phase products increases first and then decreases with the increase in reaction time, reaching its peak value at 4 h. The distribution ratio of organic carbon in gas phase products also initially increases and then decreases with the increase in reaction time, reaching its lowest value at 4 h. Considering the variations in oil and gas production rates with the increase in reaction time, it can be seen that extending reaction time could enhance both oil and gas production rates, with a stronger effect on oil production before the 4-h reaction time. Beyond the 4-h reaction time, the continued increase in reaction time further promotes gas production, accompanied by the gradual vaporization of generated oil to facilitate the migration of organic carbon in the oil production phase.

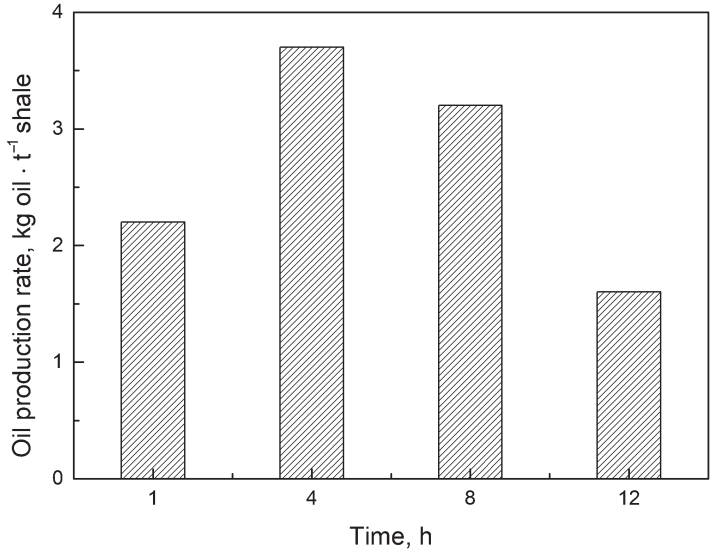

Fig. 7. Influence of time on oil production rate.

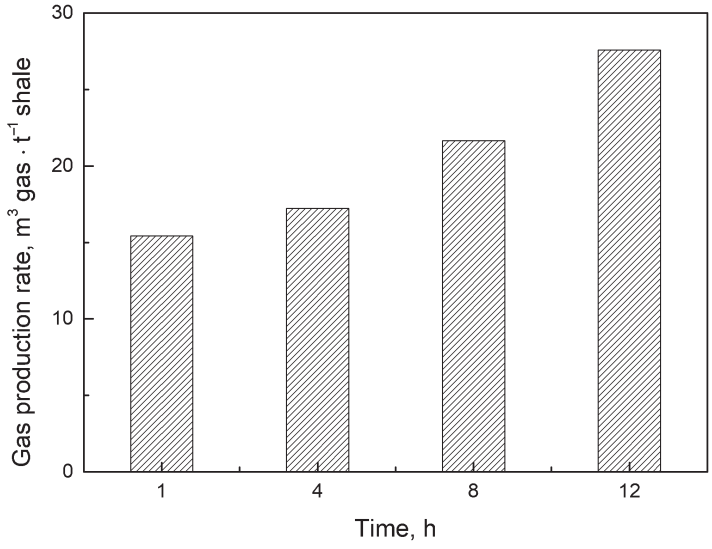

Fig. 8. Influence of time on gas production rate.

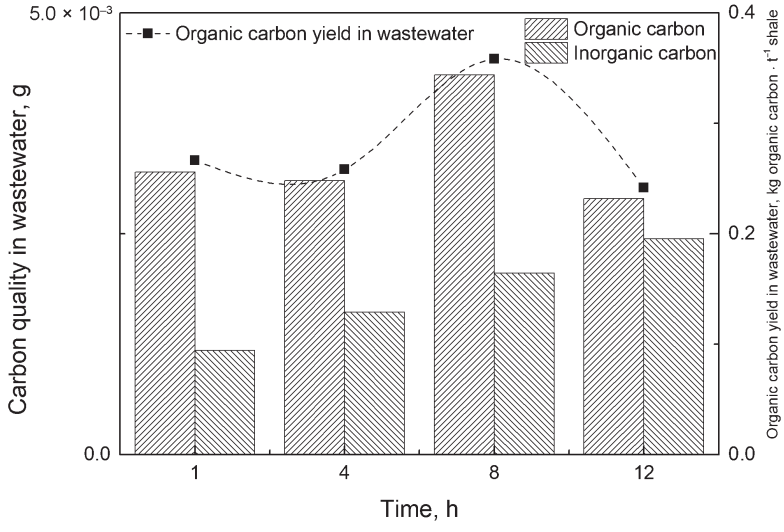

Fig. 9. Influence of time on carbon mass distribution in wastewater.

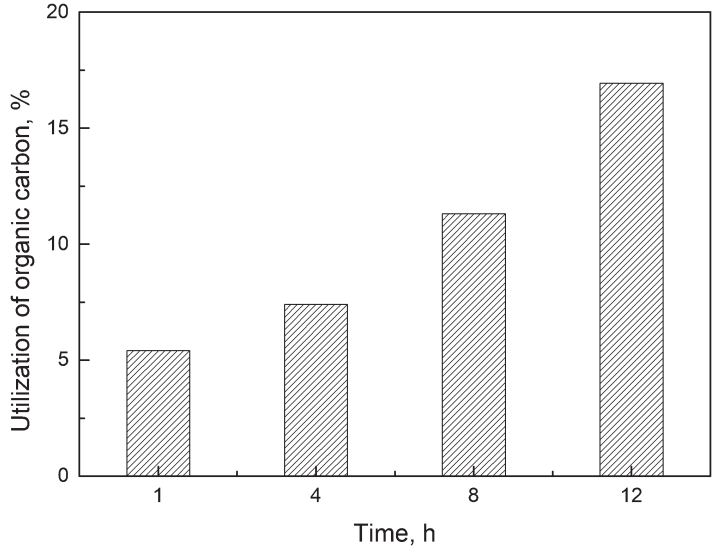

Fig. 10. Effect of time on the degree of organic carbon utilization.

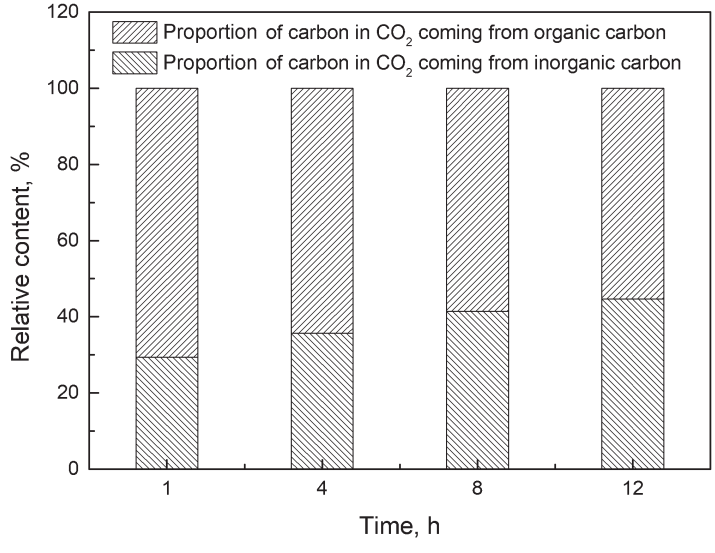

Fig. 11. Effect of time on carbon sources in carbon dioxide.

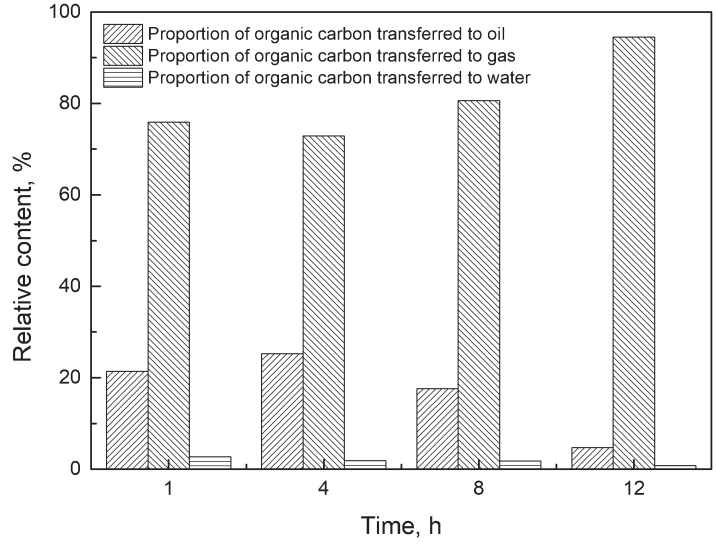

Fig. 12. Effect of time on organic carbon migration ratio.

3.2. Pore evolution

Figures 13 and 14 show the changes in mean, mode, and median pore diameters of shale after conversion in supercritical water with increasing pressure and reaction time, respectively. It is evident that the sizes of these three pore dimensions gradually decrease with the increase in pressure and gradually increase with extended reaction time. Figures 15 and 16 show the changes in porosity, permeability, and specific surface area of medium- and low-maturity organic-rich shale with varying pressure and reaction time after conversion in supercritical water, respectively. As evident, porosity, permeability and specific surface area all gradually decrease with the increase in pressure and gradually increase with extended reaction time.

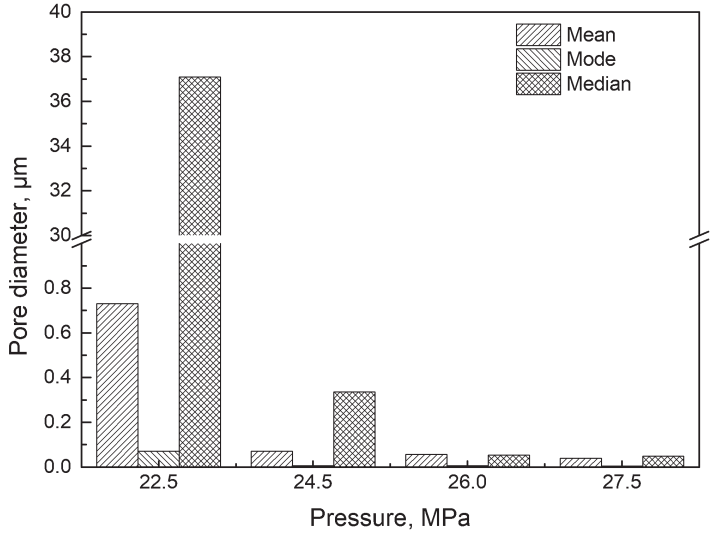

Fig. 13. Effect of pressure on pore size distribution.

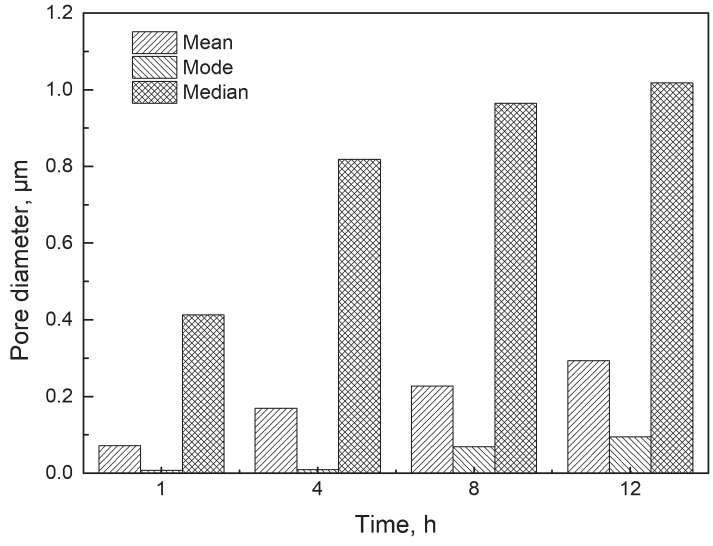

Fig. 14. Effect of reaction time on aperture distribution.

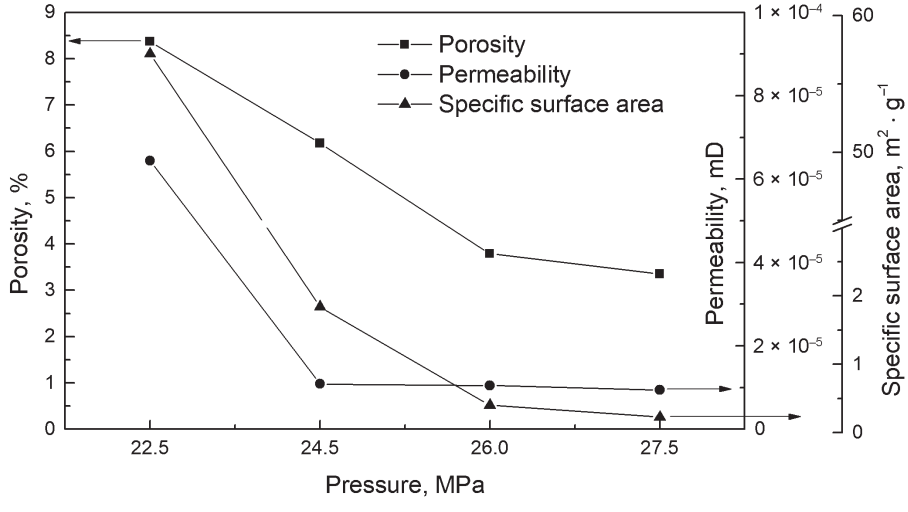

Fig. 15. Influence of pressure on porosity parameters.

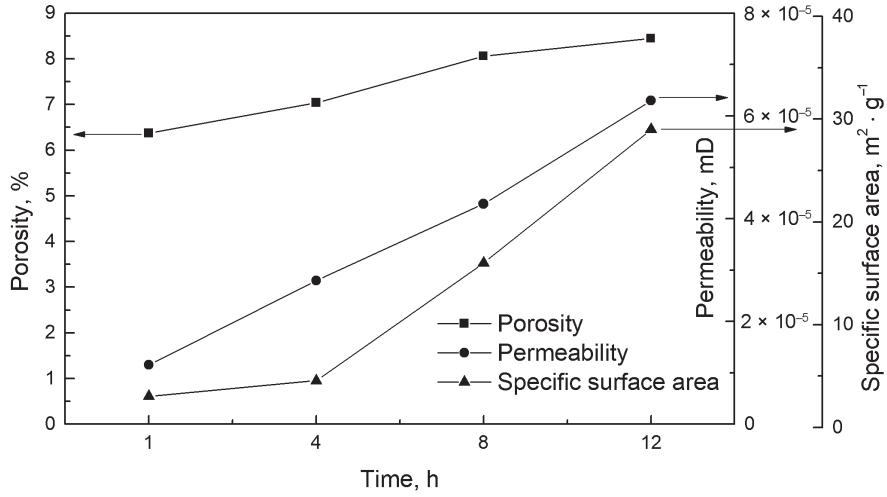

Fig. 16. Influence of reaction time on porosity parameters.

The above results show that the extension of reaction time is conducive to the expansion of pores in medium- and low-maturity organic-rich shale by supercritical water. Prolongation of reaction time leads to the pyrolysis of solid organic matter. The longer the time, the more organic matter would be converted within shale and correspondingly released. However, the increase in pressure is not conducive to the development of shale pores, so it is necessary to discuss the changes in porosity parameters under pressure in this paper.

As for the results affected by pressure factors, the hydrocarbon generation experiments conducted in this study were all conversion experiments in a static environment. The wall of the reactor cavity formed a closed boundary with constant volume, while supercritical water provided a homogeneous reaction environment in this space. The effect of supercritical water on the inside of shale was a gradual process from the outside to the inside. The interior and exterior of shale were two relatively independent spaces. The solid organic matter in the shale pores was converted into fluid dynamic organic matter under the action of heat, thereby generating pressure in the pores. Within the closed system along the inner wall of the reactor, the pore pressure inside shale constituted internal pressure, while the pressure provided by the homogeneous supercritical water environment served as external pressure.

On the one hand, increasing external pressure would increase the resistance of the dynamic organic matter in the shale's internal flow, hindering its release to the external space. On the other hand, it would cause some pores to collapse, forming dead pores. As a result, pore permeability parameters such as pore size, porosity, permeability, and specific surface area would decrease with rising pressure. In addition, the observed decrease in oil and gas production rates under the influence of increasing pressure could be attributed to the

deterioration of porosity and permeability conditions of the shale's porous medium, which impedes the smooth release of organic matter from within the shale to the external environment.

4. Conclusions

In this study, the hydrocarbon generation process of 1–4 cm sized medium- and low-maturity organic-rich shale in supercritical water was simulated using a non-isothermal heating reactor. The research focused on analyzing the effects of pressure and reaction time on the organic carbon migration path and the pore and permeability parameters to further understand the formation mechanism of shale oil and gas. Key findings from the study are the following:

1. The increase in pressure had a negative effect on the utilization of organic carbon in shale. As the pressure increased, the overall conversion efficiency of organic carbon inside the shale decreased. Although the increase in pressure could inhibit both oil and gas production, the inhibition of gas production process was more significant.
2. The effect of reaction time on oil and gas production rates varied across different stages. In the 4-h reaction time, both oil and gas production rates improved with increasing reaction time, albeit with a more significant increase observed in oil production. When reaction time exceeded 4 h, further extension of reaction time mainly promoted an increase in gas production.
3. The increase in pressure and reaction time had opposite effects on the pore structure parameters of shale. It was found that with the increase in pressure, pore structure parameters such as mean, mode, and median pore diameters, porosity, permeability and specific surface area of shale showed a decreasing trend. On the contrary, with the increase in reaction time, these pore parameters improved and expanded.

Acknowledgments

The financial support by the Basic Science Center Program of the Ordered Energy Conversion of the National Nature Science Foundation of China (grant No. 52488201) is gratefully acknowledged. The publication costs of this article were partially covered by the Estonian Academy of Sciences.

References

1. Guo, Q., Mi, S., Zhang, Q., Wang, J. Assessment methods and potential of shale oil resources in China. *Pet. Geol. Exp.*, 2023, **45**(3), 402–412.

2. Jin, Z., Bai, Z., Gao, B., Li, M. Has China ushered in the shale oil and gas revolution? *Oil Gas Geol.*, 2019, **40**(3), 451–458.
3. Zhao, W., Hu, S., Hou, L., Yang, T., Li, X., Guo, B., Yang, Z. Types and resource potential of continental shale oil in China and its boundary with tight oil. *Pet. Explor. Dev.*, 2020, **47**(1), 1–11.
4. Deng, S., Wang, Z., Gao, Y., Gu, Q., Cui, X., Wang, H. Sub-critical water extraction of bitumen from Huadian oil shale lumps. *J. Anal. Appl. Pyrolysis*, 2012, **98**, 151−158.
5. Akiya, N., Savage, P. E. Roles of water for chemical reactions in high-temperature water. *Chem. Rev.*, 2002, **102**(8), 2725−2750.
6. Bake, K. D., Pomerantz, A. E. Optical analysis of pyrolysis products of Green River oil shale. *Energy Fuels*, 2017, **31**(12), 13345−13352.
7. Kang, Z., Zhao, Y., Yang, D. Review of oil shale in-situ conversion technology. *Appl. Energy*, 2020, **269**, 115121.
8. Tang, X., Li, S., Yue, C., He, J., Hou, J. Lumping kinetics of hydrodesulfurization and hydrodenitrogenation of the middle distillate from Chinese shale oil. *Oil Shale*, 2013, **30**(4), 517−535.
9. Lewan, M. D. Water as a source of hydrogen and oxygen in petroleum formation by hydrous pyrolysis. *Prepr. Pap. – Am. Chem. Soc., Div. Fuel Chem.*, 1992, **37**, 1643−1649.
10. Hou, L., Ma, W., Luo, X., Liu, J. Characteristics and quantitative models for hydrocarbon generation-retention-production of shale under ICP conditions: example from the Chang 7 member in the Ordos Basin. *Fuel*, 2020, **279**, 118497.
11. Xie, T., Zhao, Q., Jin, H., Wang, Y., Guo, L. Reaction kinetics study on hydrocarbon generation of medium- and low-maturity organic-rich shale in supercritical water. *Energy Fuels*, 2023, **37**(18), 14192–14201.
12. Xie, T., Zhao, Q., Jin, H., Wang, Y., Guo, L. Experimental investigation on the organic carbon migration path and pore evolution during co-thermal hydrocarbon generation of low maturity organic-rich shale and supercritical water. *Energy Fuels*, 2022, **36**(24), 15047–15054.
13. Weingärtner, H., Franck, E. U. Supercritical water as a solvent. *Angew. Chem. Int. Ed.*, 2005, **44**(18), 2672−2692.
14. Zhao, Q., Guo, L., Huang, Z., Chen, L., Jin, H., Wang, Y. Experimental investigation on enhanced oil recovery of extra heavy oil by supercritical water flooding. *Energy Fuels*, 2018, **32**(2), 1685−1692.
15. Jin, H., Guo, L., Guo, J., Ge, Z., Cao, C., Lu, Y. Study on gasification kinetics of hydrogen production from lignite in supercritical water. *Int. J. Hydrog. Energy*, 2015, **40**(24), 7523−7529.
16. Kruse, A. Supercritical water gasification. *Biofuels Bioprod. Biorefin.*, 2008, **2**(5), 415−437.
17. Reddy, S. N., Nanda, S., Dalai, A. K., Kozinski, J. A. Supercritical water gasification of biomass for hydrogen production. *Int. J. Hydrog. Energy*, 2014, **39**(13), 6912−6926.
18. Rodriguez Correa, C., Kruse, A. Supercritical water gasification of biomass for

hydrogen production – review. *J. Supercrit. Fluids*, 2018, **133**(2), 573−590.
19. Guo, L., Jin, H., Lu, Y. Supercritical water gasification research and development in China. *J. Supercrit. Fluids*, 2015, **96**, 144−150.
20. Rana, R., Nanda, S., Kozinski, J. A., Dalai, A. K. Investigating the applicability of Athabasca bitumen as a feedstock for hydrogen production through catalytic supercritical water gasification. *J. Environ. Chem. Eng.*, 2018, **6**(1), 182−189.
21. Rana, R., Nanda, S., Maclennan, A., Hu, Y., Kozinski, J. A., Dalai, A. K. Comparative evaluation for catalytic gasification of petroleum coke and asphaltene in subcritical and supercritical water. *J. Energy Chem.*, 2019, **31**, 107−118.
22. García-Jarana, M. B., Sánchez-Oneto, J., Portela, J. R., Martínez de la Ossa, E. J. Supercritical water gasification of organic wastes for energy generation. In: *Supercritical Fluid Technology for Energy and Environmental Applications* (Anikeev, V., Fan, M., eds). Elsevier, Boston, 2014, 191−200.
23. Cao, C., Zhang, Y., Li, L., Wei, W., Wang, G., Bian, C. Supercritical water gasification of black liquor with wheat straw as the supplementary energy resource. *Int. J. Hydrog. Energy*, 2019, **44**(30), 15737−15745.
24. Wang, C., Zhu, C., Huang, J., Li, L., Jin, H. Enhancement of depolymerization slag gasification in supercritical water and its gasification performance in fluidized bed reactor. *Renew. Energy*, 2021, **168**(21), 829−837.
25. Veski, R., Palu, V., Kruusement, K. Co-liquefaction of kukersite oil shale and pine wood in supercritical water. *Oil Shale*, 2006, **23**(3), 236−248.
26. Funazukuri, T., Yokoi, S., Wakao, N. Supercritical fluid extraction of Chinese Maoming oil shale with water and toluene. *Fuel*, 1988, **67**(1), 10–14.
27. Yanik, J., Yüksel, M., Sağlam, M., Olukçu, N., Bartle, K., Frere, B. Characterization of the oil fractions of shale oil obtained by pyrolysis and supercritical water extraction. *Fuel*, 1995, **74**(1), 46–50.
28. El Harfi, K., Bennouna, C., Mokhlisse, A., Ben Chanâa, M., Lemée, L., Joffre, J., Amblès, A. Supercritical fluid extraction of Moroccan (Timahdit) oil shale with water. *J. Anal. Appl. Pyrolysis*, 1999, **50**(2), 163–174.
29. Liang, X., Zhao, Q., Dong, Y., Guo, L., Jin, Z., Liu, Q. Experimental investigation on supercritical water gasification of organic-rich shale with low maturity for syngas production. *Energy Fuels*, 2021, **35**(9), 7657–7665.
30. Hu, H., Zhang, J., Guo, S., Chen, G. Extraction of Huadian oil shale with water in sub- and supercritical states. *Fuel*, 1999, **78**(6), 645–651.
31. Nasyrova, Z. R., Kayukova, G. P., Onishchenko, Y. V., Morozov, V. P., Vakhin, A. V. Conversion of high-carbon domanic shale in sub- and supercritical waters. *Energy Fuels*, 2020, **34**(2), 1329–1336.
32. Xie, T., Zhao, Q., Dong, Y., Jin, H., Wang, Y., Guo, L. Experimental investigation on the hydrocarbon generation of low maturity organic-rich shale in supercritical water. *Oil Shale*, 2022, **39**(3), 169–188.
33. Sun, Y., Kang, S., Wang, S., He, L., Guo, W., Li, Q., Deng, S. Subcritical water extraction of Huadian oil shale at 300 °C. *Energy Fuels*, 2019, **33**(3), 2106–2114.